

Theoretical study of electron transport in boron nanotubes

Kah Chun Lau, Ravindra Pandey,^{a)} and Ranjit Pati

Department of Physics and Multi-Scale Technology Institute, Michigan Technological University,
Houghton, Michigan 49931

Shashi P. Karna

U.S. Army Research Laboratory, Weapons and Materials Research Directorate, AMSRD-ARL-WM,
Aberdeen Proving Ground, Maryland 21005-5069

(Received 18 January 2006; accepted 13 April 2006; published online 25 May 2006)

The electron transport in single-walled boron nanotube (BNT) is studied using the Landauer-Büttiker [R. Landauer, *J. Phys.: Condens. Matter* **1**, 8099 (1989); M. Büttiker, *Phys. Rev. Lett.* **57**, 1761 (1986)] multichannel approach in conjunction with the tight-binding method. In the range of the calculated length (1–5.0 nm) of the tubes, the calculations predict a ballistic transport in BNT and find a relatively low resistance for BNTs as compared to that of the single-walled carbon nanotubes (CNTs) of comparable length. A lower resistance in the case of BNT than the CNT may be attributed to electron-deficient nature of boron characterized by the presence of two-center, and multicenter bonds in the former. © 2006 American Institute of Physics. [DOI: 10.1063/1.2207570]

An ever increasing need for smaller, denser, and faster processors has led to focus efforts toward developing and identifying novel one-dimensional (1D) systems as the basic building blocks for nanoscale electronic devices. Among others, the carbon nanotubes (CNTs) have emerged as prototypical 1D system and have been the subject of intense research in recent years for their applications in nanoelectronics.¹ However, despite their excellent mechanical and electrical characteristics, the CNTs suffer from serious limitations due to a lack of the availability of high-purity materials.² Therefore, attention is now turned to alternatives to CNTs that can be bulk produced in high purity and can be easily processed and integrated with existing Si-based processes. Toward that, elemental boron nanotubes (BNTs) are recognized as a potential candidate material due to their electron deficient character.^{3–5} A recent experiment⁶ reporting the synthesis of single-wall (SW) boron nanotubes has further evoked the interest and expectations for their applications in nanoelectronics.

In this letter, we report the results of our quantum mechanical study of electron transport in SWBNTs using the Landauer-Büttiker multichannel approach^{7–9} in conjunction with a tight-binding model. We note here that a number of theoretical studies^{10–13} were directed toward understanding the formation and structure of BNTs. Our calculated results find a higher conductivity associated with SWBNT relative to the conductivity of SWCNT of similar geometry. Furthermore, our calculations suggest that between 1 and 5.0 nm, the electron transport in a BNT is ballistic in nature.

In a previous theoretical study,¹³ it was shown that, similar to the carbon nanotubes, two different chiral structures, namely, zigzag (type I) and armchair (type II), can be constructed from two-dimensional (2D) planar sheets of boron. Our first-principles density functional theory (DFT) calculations¹³ predicted the SWBNT with type I (zigzag) to be more stable than the type II (armchair). In the present study, the geometry of the SWBNT was taken from our previous work.¹³ The geometrical arrangement used to calculate

the electrical properties of the SWBNT is shown in Fig. 1. In brief, a SWBNT with varying length was sandwiched between gold electrodes represented by a single layer consisting of 49 Au atoms at each side. In order to test the convergence of calculated current with respect to the placement of the equilibrium Fermi level, the number of the Au layers was varied from one to six at each side, as shown in Fig. 1. The Au layers were separated by 2.16 Å.¹⁴ For a 35 Å long SWBNT, the calculated current and E_F of Au (one layer)-SWBNT-Au (one layer) converged within ~7.5% and ~1.3% with respect to Au (six layers)-SWBNT-Au (six layers), when E_F was placed in the middle of the highest occupied molecular orbital (HOMO) and the lowest unoccupied molecular orbital (LUMO) of the nanotube-Au system. In the subsequent calculations, we therefore place the equilibrium Fermi level E_F in the middle of the HOMO and the LUMO of the Au (one layer)-SWNT-Au (one layer) system. The Au-B separation at the electrode-tube interface was taken to be 1.7 Å, which is approximately the calculated equilibrium distance for diatomic Au-B.¹⁵

The current (I)-voltage (V) characteristics of SWBNT were calculated by the nonequilibrium Green's function method,⁹ utilizing the Landauer-Büttiker formalism as^{7–9,16}

$$I = \frac{2e}{h} \int_{E_F - eV/2}^{E_F + eV/2} T(E, V) [f(E, E_F - eV/2) - f(E, E_F + eV/2)] dE. \quad (1)$$

In Eq. (1), $T(E, V)$ is the transmission function, E is the

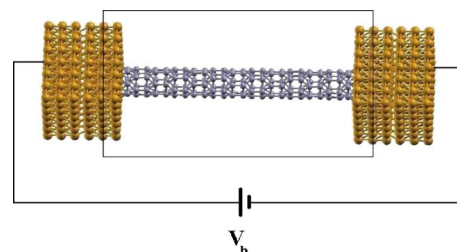


FIG. 1. (Color online) A schematic diagram of two probe device architecture with SWBNT sandwiched between two gold electrodes. The region with the rectangular box is taken to be the simulation cell for transport calculations.

^{a)}Electronic mail: pandey@mtu.edu

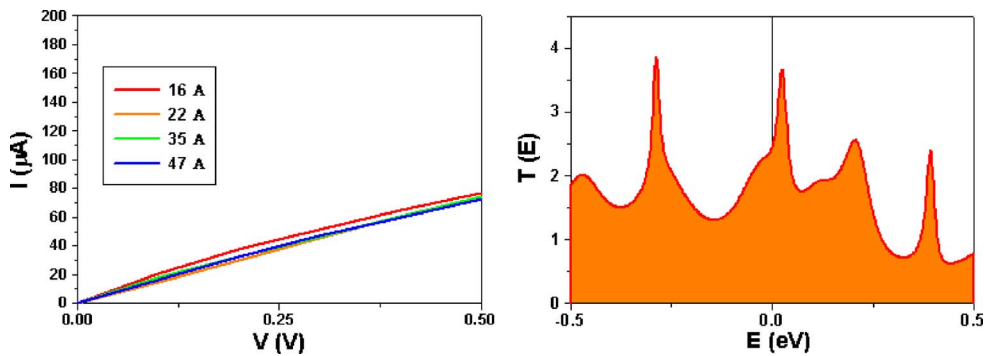


FIG. 2. (Color online) I - V characteristics of type-I (6,0) SWBNT in a strong gold-nanotube-gold coupling regime, with the corresponding figures showing the transmission spectra of the system.

injection energy, and E_F represents the Fermi energy of Au. The transmission function $T(E, V)$ is calculated as

$$T(E, V) = \text{Tr}\{\Gamma_L G^R \Gamma_R G^A\}. \quad (2)$$

The Green's function G^R in the present study was obtained in the framework of nonorthogonal tight-binding model. Four valence (s , p_x , p_y , p_z) orbitals for the boron and one s orbital for the gold atom were included in the calculation.

The calculated I - V characteristics for (6,0) SWBNT of different lengths between 16 and 47 Å are shown in Fig. 2. Also shown in Fig. 2 is the transmission spectrum for a 35 Å SWBNT. The transmission spectra mimic the shape of density of states (not shown here). It should be mentioned that the qualitative features of density of states of the metallic (6,0) SWBNT calculated in the present study agree very well with those calculated from the first-principles methods.¹³ It is clear from Fig. 2 that the calculated current in SWBNT is independent of the length of the tube, indicative of the ballistic nature of electron transport.

In order to verify the accuracy of the predicted results for SWBNT, for which no data exist for comparison, we performed similar calculations on metallic SWCNT, for which experimental and theoretical data exist.¹⁷⁻²³ Calculations were performed in the similar geometry, as shown for the SWBNT in Fig. 1. In the case of SWCNT, the configuration was taken to be that of armchair (6,6) SWCNT and the electrodes were represented by 81 Au atoms per layer on each side. The C-Au distance at the metal-molecule interface was taken to be 1.7 Å as approximately the calculated equilibrium geometry for Au-C dimer.¹⁵ As in the case of SWBNT, we take this distance as the strong coupling regime between electrode and nanotube. The calculated I - V characteristics of (6,6) SWCNT of varying lengths between 10 and 53 Å along with the transmission spectrum for one of the tubes (of 26 Å length) are shown in Fig. 3.

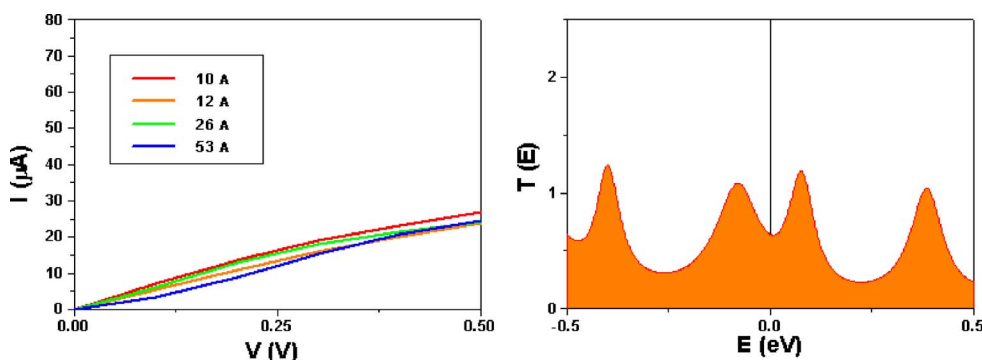


FIG. 3. (Color online) I - V characteristics of (6,6) SWCNT in a strong gold-nanotube-gold coupling regime, with the corresponding figures showing the transmission spectra of the system.

As evident from the figure, the present calculations clearly show a length-independent I - V characteristic for SWCNT, as known from previous experimental and theoretical studies.¹⁷⁻²³ This gives confidence in our calculations and predicted results for SWBNT. The resistance of SWBNT is estimated to be 7 kΩ to be compared with the corresponding value of ~20 kΩ for SWCNT. The corresponding equilibrium conductance of SWBNT is $\sim 2G_0$, where $G_0 = 2e^2/h$ (unit of quantum conductance) near the Fermi level. It was determined from first-principles band structure calculations.¹³

The calculated difference in total resistance between the gold-BNT-gold and gold-CNT-gold systems therefore appears to be due to their respective contact resistances. An analysis of transmission spectra given in Figs. 2 and 3, respectively, suggests that both subbands of (6,0) type-I SWBNT carrying current couple well to the metal as compared to only one of the two subbands of (6,6) SWCNT due to the scattering at the interface. This difference perhaps accounts for the calculated difference in the conductance of SWBNT and SWCNT (Fig. 4).

Further understanding of the conductance in SWBNT can be obtained from an analysis of the nature of the chemical bonds. In our previous study,¹³ it was noted that the bonding in (6,0) SWBNT can be described as mixed metallic and covalent types, in contrast to sp^2 -type covalent bonding in the (6,6) SWCNT. Thus, we believe that a mixture of two-center, directional covalent (σ -type) bonds along the tube axis and multicenter bonds along the circumference of the tube provides conduction channels for the electron transport in BNTs. Calculations using state-of-the-art real space, non-equilibrium Green's function (NEGF) formalism combined with DFT based simulation²⁴ are in progress to confirm the role played by the bonding in the electron transport in BNTs relative to CNTs.

It is important to note that in addition to the bonding features and electronic structures of the nanotubes, the nature

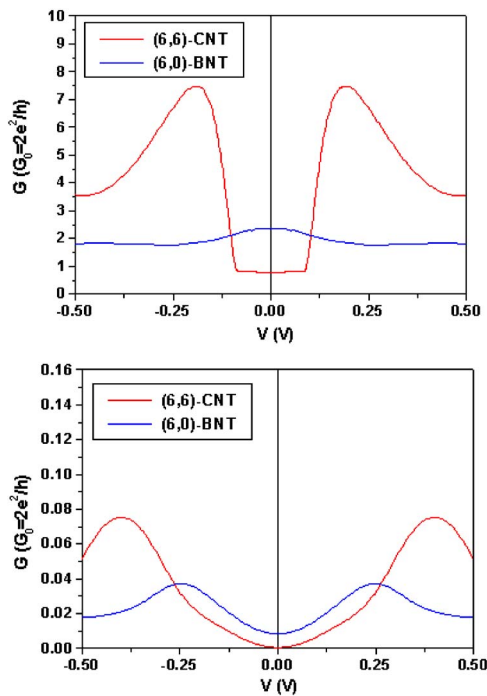


FIG. 4. (Color online) Conductance (G) of (6,6) SWCNT and type-I (6,0) SWBNT in strong (top) and weak (bottom) gold-nanotube-gold coupling regime.

of the metal-tube contact can also influence the calculated/observed resistance of the system. Our calculations suggest that the contact resistance can also be altered by changing $R_{\text{interface}}$ (i.e., Au-NT separation at the gold electrode-tube interface) from 1.7 to 3.5 Å. In both Au-CNT-Au and Au-BNT-Au systems, a significant decrease in magnitude of current together with a nonlinear variation of current with applied bias is seen. In the strong coupling regime ($R_{\text{interface}} = 1.7$ Å) at 0.5 V, a significantly higher current was predicted in both BNT and CNT-systems, as compared to that in the weak coupling regime ($R_{\text{interface}} = 3.5$ Å) at 0.5 V. The decrease in current in the weak coupling regime may be attributed to a shift of the Fermi energy toward the valence band, leading to a higher resistance relative to the case of the strong coupling regime where the Fermi energy shifts toward the conduction band. Also, the discretized energy spectra in density of states of gold-nanotube-gold systems may be attributed to the predicted nonlinear I - V characteristics in the weak gold-nanotube-gold coupling regime.

In order to gain further insights into the electron transport in nanotubes, we have calculated the conductance (G) in both the cases of strong and weak coupling regimes (Fig. 4). In the strong coupling regime, a strong oscillation in conductance (i.e., dI/dV) is predicted for CNT as compared to a nearly constant slope in current for BNT, indicating its Ohmic-like I - V characteristics. A similar feature in conductance for BNT relative to CNT is predicted in the weak coupling regime.

Finally, we consider metallic type-II (0,6) SWBNT for electron transport calculations to explore the effect of chirality on the I - V characteristics. The calculated results suggest that chirality does not appear to play a significant role in determining the I - V characteristics of (0,6) SWBNT. It can

be attributed to the similarity of bonding features in (6,0) and (0,6) SWBNTs as noted in our previous study.¹³

In summary, we have calculated the I - V characteristics of (6,0) and (0,6) SWBNTs using tight-binding approach and the Landauer-Büttiker multichannel formalism. The calculations predict a ballistic nature of electron transport in SWBNT. Furthermore, the conductivity in SWBNT is calculated to be higher than that in SWCNT, which is attributed to a mixture of localized two-center bonds and delocalized multicenter electron-deficient nature of boron bonds in SWBNT. Metal-tube interface coupling appears to strongly influence the I - V characteristics of the nanotubes. The chirality of boron nanotubes does not appear to play a significant role in determining the I - V characteristics of a BNT. The present study is expected to stimulate further investigations of electronic properties in BNTs.

The work at Michigan Technological University was performed under support by the DARPA through Contract No. ARL-DAAD17-03-C-0115. The work at Army Research Laboratory (ARL) was supported by the DARPA MoleApps program and ARL Director's Research Initiative FY05-WMR01. Fruitful discussions with Professor Hong Guo are gratefully acknowledged.

¹R. Saito, G. Dresselhaus, and M. S. Dresselhaus, *Physical Properties of Carbon Nanotubes* (Imperial College Press, London, 2003).

²Y. Xu, H. Peng, R. H. Hauge, and R. E. Smalley, *Nano Lett.* **5**, 163 (2005).

³E. L. Muetterties, *The Chemistry of Boron and its Compounds* (Wiley, New York, 1967).

⁴T. T. Xu, J. Zheng, N. Wu, A. W. Nicholls, J. R. Roth, D. A. Dikin, and R. S. Ruoff, *Nano Lett.* **4**, 963 (2004).

⁵D. Wang, J. G. Lu, C. J. Otten, and W. E. Buhro, *Appl. Phys. Lett.* **83**, 5280 (2003).

⁶D. Ciuparu, R. F. Klie, Y. Zhu, and L. Pfefferle, *J. Phys. Chem. B* **108**, 3967 (2004).

⁷R. Landauer, *J. Phys.: Condens. Matter* **1**, 8099 (1989).

⁸M. Büttiker, *Phys. Rev. Lett.* **57**, 1761 (1986).

⁹S. Datta, *Electronic Transport Properties in Mesoscopic Systems* (Cambridge University Press, Cambridge, 1995).

¹⁰A. Gindulyte, W. N. Lipscomb, and L. Massa, *Inorg. Chem.* **37**, 6544 (1998).

¹¹I. Boustani, A. Quandt, E. Hernández, and A. Rubio, *J. Chem. Phys.* **110**, 3176 (1999).

¹²M. H. Evans, J. D. Joannopoulos, and S. T. Pantelides, *Phys. Rev. B* **72**, 045434 (2005).

¹³K. C. Lau, R. Pati, R. Pandey, and A. C. Pineda, *Chem. Phys. Lett.* **41**, 549 (2006).

¹⁴C. Kittel, *Introduction to Solid State Physics* (Wiley, New Delhi, India, 1993).

¹⁵DFT calculations find the equilibrium distances for Au-B and Au-C dimers to be 1.98 and 1.93 Å.

¹⁶R. Pati, Y. Zhang, S. K. Nayak, and P. M. Ajayan, *Appl. Phys. Lett.* **81**, 2638 (2002).

¹⁷S. J. Tans, M. H. Devoret, H. Dai, A. Thess, R. E. Smalley, L. J. Geerligs, and C. Dekker, *Nature (London)* **386**, 474 (1997).

¹⁸A. Bachtold, M. S. Fuhrer, S. Plyasunov, M. Forero, E. H. Anderson, A. Zettl, and P. L. McEuen, *Phys. Rev. Lett.* **84**, 6082 (2000).

¹⁹V. Krstić, S. Roth, and M. Burghard, *Phys. Rev. B* **62**, R16353 (2000).

²⁰W. Liang, M. Bockrath, D. Bozovic, J. Hafner, M. Tinkham, and H. Park, *Nature (London)* **411**, 665 (2001).

²¹J. Kong, E. Yenilmez, T. W. Tombler, W. Kim, H. Dai, R. B. Laughlin, L. Liu, C. S. Jayanthi, and S. Y. Wu, *Phys. Rev. Lett.* **87**, 106801 (2001).

²²C. T. White and T. N. Todorov, *Nature (London)* **393**, 240 (1998).

²³M. P. Anantram and T. R. Govindan, *Phys. Rev. B* **58**, 4882 (1998).

²⁴J. Taylor, H. Guo, and J. Wang, *Phys. Rev. B* **63**, 121104 (2001).